View metadata, citation and similar papers at core.ac.uk

brought to you by CORE

provided by Online Research Database In Technology

Technical University of Denmark

Comparison of two finite element methods with experiments of delaminated composite panels

Branner, Kim; Berring, Peter; Gaiotti, M.; Rizzo, C.M.

Published in:
Proceedings

Publication date:
2011

Link back to DTU Orbit

Citation (APA):
Branner, K., Berring, P., Gaiotti, M., & Rizzo, C. M. (2011). Comparison of two finite element methods with experiments of delaminated composite panels. In Proceedings

DTU Library
Technical Information Center of Denmark

General rights
Copyright and moral rights for the publications made accessible in the public portal are retained by the authors and/or other copyright owners and it is a condition of accessing publications that users recognise and abide by the legal requirements associated with these rights.

- Users may download and print one copy of any publication from the public portal for the purpose of private study or research.
- You may not further distribute the material or use it for any profit-making activity or commercial gain
- You may freely distribute the URL identifying the publication in the public portal

If you believe that this document breaches copyright please contact us providing details, and we will remove access to the work immediately and investigate your claim.

COMPARISON OF TWO FINITE ELEMENT METHODS WITH EXPERIMENTS OF DELAMINATED COMPOSITE PANELS

K. Branner[1]*, P. Berring[1], M. Gaiotti[2] & C. M. Rizzo[2]
[1] Risø National Laboratory for Sustainable Energy, Technical University of Denmark, Denmark
[2] DINAEL, Faculty of Engineering, University of Genoa, Italy
* Corresponding author (kibr@risoe.dtu.dk)

Keywords: *Compressive Strength, Delamination, Finite Element Analysis, Experiments*

1 Introduction

This paper focuses on two different modeling approaches for delaminated multilayer composite panels: The former, applied by Risø DTU, adopts 20-node orthotropic solid elements with 3 degrees of freedom (DOF) per node, and the latter, developed by the University of Genoa, adopts shell elements with 6 DOF per node.

The results obtained from the two finite element modeling methods are compared with experimental results from testing flat composite panels with and without delaminations.

The aim of this work is to eventually compare the finite element results with the experimental data in order to discuss pros and cons for the modeling methods and to provide suggestions for reliable prediction of consequences of delaminations in thick composite panels.

2 Numerical Modeling Approaches

The panels modeled are relatively thick with a thickness to width ratio of about 0.067. They consist entirely of unidirectional (UD) layers with all fibers in the loading direction and are somewhat similar to the load carrying laminates in a typical wind turbine blade, where approximately 90% of the fibers are in the lengthwise direction.

Mechanical properties representative of unidirectional fiber glass laminates produced in the laboratory is used in this work, see Hansen et al. [1]:

E_{11}=46.5GPa	G_{12}=4.1GPa	ν_{12}=0.25
E_{22}=13.4GPa	G_{23}=2.6GPa	ν_{23}=0.25

The plate taken into account for the numerical analysis is rectangular with an aspect ratio A/B=1.36 where A is the length of the edge along the load direction, having the same orientation of the fibers. Corresponding lower case letters (a, b) are used to define the delamination size, having the same aspect ratio of the panel. See Fig. 1 for size definitions.

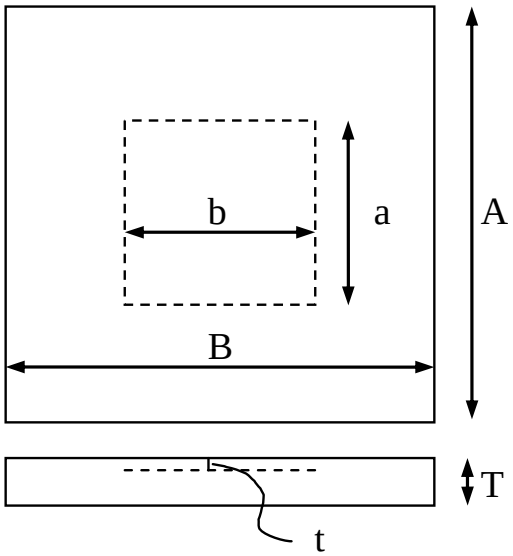

Fig. 1. Definition of panel and delamination geometry.

2.1 Solid Elements Model

The 3D solid finite element models were modeled with 20-node orthotropic elements. Two or three elements were used through the thickness depending on the through thickness position of the delamination.

A small out-of-plane displacement corresponding to the first buckling mode shape was applied as an initial imperfection of the delaminated sublaminate. The amplitude of the initial imperfections was approximately 0.5‰ of the panel thickness.

The elements were all joined in the interfaces (nodes coincidence), except for the delaminated area where quadratic contact conditions were applied to

prevent penetration. The panel is considered simply supported in the midline of all its edges. Therefore all panel models have nodes at these midlines. The load is applied by forcing a uniform in-place displacement on one of the short edges and constraining the opposite edge (B edges in Fig. 1).

The average number of degrees of freedom (DOFs) was approximately 150.000. Nonlinear geometric analyses were conducted using an implicit solution algorithm.

2.2 Shell Elements Model

The shell element model presented in this paper is defined by a single shell surface for the intact path and by two surfaces for the delaminated area, each surface representing one side of the delamination, as shown in Fig. 2.

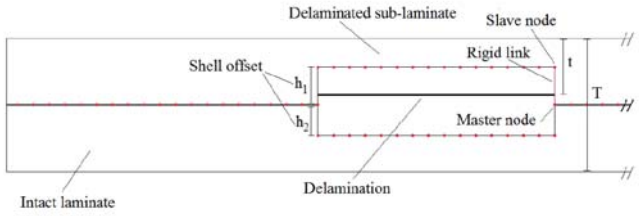

Fig. 2. Rigid link coupling between intact and delaminated path, master and slave nodes positions.

The nodes along the edge of the delamination are coupled to the nodes on the main surface by a rigid link constraint, where the master node is the node lying on the edge of the intact middle plane and the nodes on both sub laminates edges are its slaves.

A 9-nodes shell elements mesh has been generated on the surfaces, for a total number of about 4800 elements; the element type is the MITC9 as suggested in [2], to prevent element locking problems for thin laminates. To avoid penetrations between the surfaces defining the sub laminates in the delaminated area, a contact algorithm has been taken into account. The panel is considered simply supported on all its edges; a distributed compressive line load is applied on the short edges.

See [3] for a more detailed description of the numerical modeling approaches.

2.3 Delamination Modes

Different behavior can be observed when a delaminated panel is subjected to compressive in-plane load and this behavior depends on delamination size and position. Typically two different behaviors are expected: Global mode buckling, where the sub laminates on both sides of the delamination moves to the same side, and local mode buckling where the sub laminates move towards opposite sides. As observed by Peck and Springer [4], when local buckling occurs, it introduces bending in the plies on the other side of the delamination, so that they are subjected to both bending and compressive stress resulting in a reduced failure load.

However, results from the 3D solid models also show that combinations of the global and local modes can appear as so-called combined modes or sub-modes. The sub-modes are found to appear for special combination of delamination size and through thickness position. In these studies five different mode types have been observed.

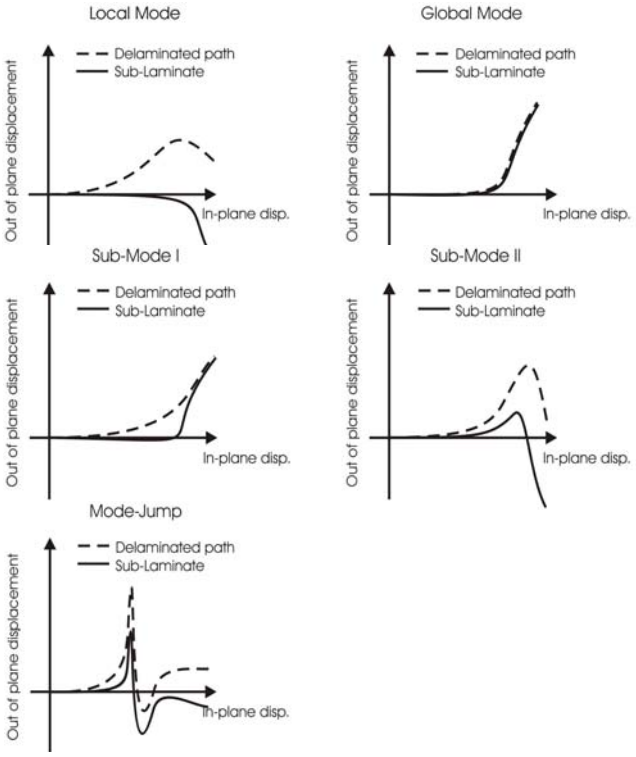

Fig. 3. Delamination modes shown with the corresponding central out-of-plane displacement for the two delaminated sub-laminates.

These modes are illustrated in Fig. 3, where the relation between the out-of-plane displacements at the centre of the two delaminated sub-laminates is plotted.

The buckling map shown in Fig. 4 is divided into the following 3 areas:

- Local buckling, occurring for large delaminations close to the surface,
- Global buckling, occurring for small and deep delaminations,
- Sub-mode, occurring for large and deep delaminations.

The buckling mode map is similar to those reported by Short et al. [5]. However, in [5] only local and global modes were considered.

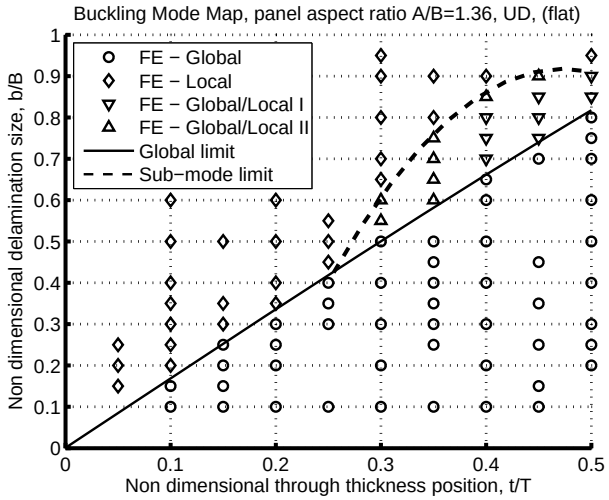

Fig. 4. Buckling mode map for a 100% unidirectional fiber composite laminate. From [7].

2.4 Panel Strength

Both in the numerical and experimental studies, the ultimate strength of the panels are defined using a robust method to define buckling that was proposed in [7].

The normalized in-plane force is plotted against the normalized in-plane displacement. In the start of the load history, the response of the panels is linear, but as the panels start to buckle, the response becomes non-linear.

A linear curve is determined by the first 30% of this load history and then offset by 2.5%. The buckling load is then found as the load at the intersection between this linear curve and a spline interpolation of the entire load history, see Fig. 5.

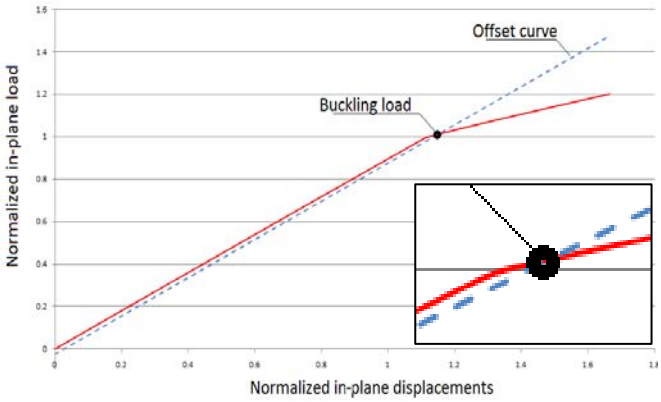

Fig. 5. Robust method to define buckling load in non-linear analysis.

Applying this method to determine the critical load, the buckling strength normalized with respect to the critical load for the intact panel is calculated as function of the delamination size and its through-thickness position.

Using numerical interpolations it is then possible to produce the strength reduction maps shown in Fig. 6, where results are reported for the two adopted finite element strategies.

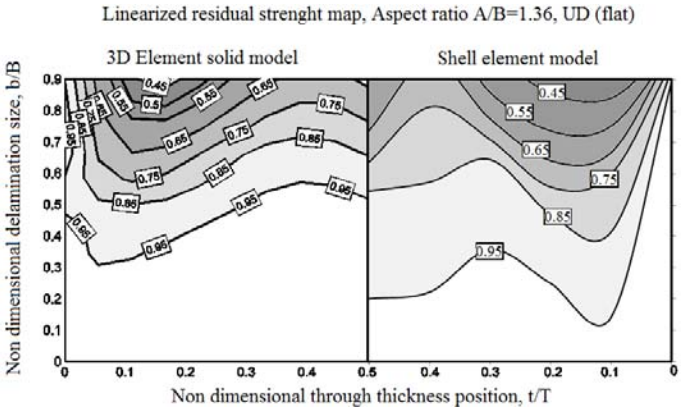

Fig. 6. Reduced compressive strength map for the solid and shell element models respectively, see [3]. Note that the maps are mirrored with respect to the y-axis for sake of easier comparison.

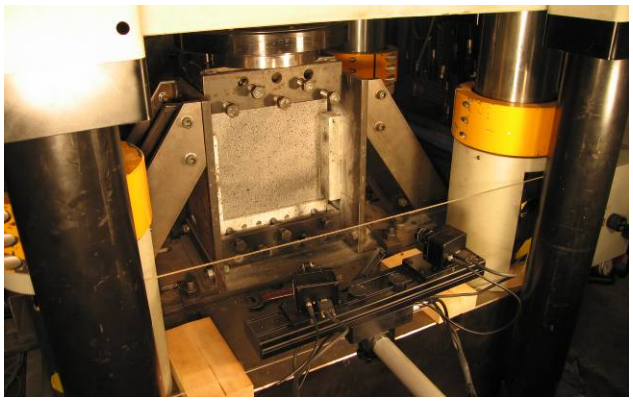

Fig. 7. Experimental setup. Deflections were measured by a DIC measurement system on one side of the panel and by conventional displacement transducers on the other side.

3 Experimental Results

A large number of flat composite panels with and without delaminations have been tested until failure as reported in [6-7].

The test specimens are approximately 400x380x20 mm rectangular composite panels made of glass fiber reinforcement plastic. The lay-up is symmetric with approximately 90% of the reinforcement in the load direction and the remaining reinforcement in the ±45º directions. Two different types of panels were tested. One type (Pr) was made with prepregs and the other type (In) was made using the vacuum infusion technique. Even though the specimens were made similar to the load carrying laminate in a typical wind turbine blade, the material properties are not fully representative to those in real wind turbine blades, as the specimens were produced in a lab under different conditions.

For both types, some of the panels were manufactured with no intentional defects or imperfections, while others had Teflon sheets embedded to simulate delaminated rectangular areas of different size and depth. A specially designed test rig (see [6]) was used in a 5 MN Instron testing machine as shown in Fig. 7. The rig is designed to limit rotation and out-of-plane deflection of the edges of the panels. The panels were loaded to ultimate failure and a digital image correlation (DIC) measurement system was used in addition to conventional displacement transducers to monitor full field displacements of the panels under increasing load.

As described above, the compressive loaded panels are subjected to the two different buckling modes; the global buckling mode and the local buckling mode. The following buckling responses were observed during the experiments:

a) Global buckling.
b) Local buckling without growth. The delaminated zone pops out and very little growth of the delaminated zone is observed before ultimate failure.
c) Local buckling with growth. The delaminated zone pops out and substantial growth of the delaminated zone is observed before ultimate failure.
d) Global buckling with mode jump. The buckling begins in the 1st global mode shape. At failure a mode-jump is observed and the panel fails in an s-shape.
e) Local buckling cause instant failure. The panel fails right after the delaminated zone pops out. This typically occurs at high loading.

The buckling load was determined for each panel using the robust method described in the previous section. The average buckling loads for the small series of each type is denoted P_i and the average buckling loads for panels without delaminations is denoted P_n. The two different panel types with respect to manufacturing process were treated separately meaning that they have different P_n.

Table 1 lists the main results from the experimental panel tests. The panels have delaminations of different size and through thickness position. For a few of the panels, strange behavior was observed or measuring equipment was not running properly. These panels are not included here. In Table 1, average results are shown for between 2 and 4 specimens of each type.

Table 1. Tests results: the prevailing observed buckling mode is listed together with the measured reduced strength, i.e. ratio between average buckling load of delaminated panel (P_i) by average buckling load of non delaminated panel (P_n).

Test panels					**Failure**	
Code	Specimens	a/A	b/B	t/T	Type	P_i/P_n
In 4	2		None		Global	100%
In 5a	3	0,48	0,39	0,31	Global	81%
In 5b	4	0,47	0,39	0,21	Local	87%
In 6a	2	0,36	0,30	0,31	Global	87%
In 6b	4	0,35	0,30	0,21	Local	83%
In 7a	2	0,42	0,34	0,25	Global	92%
In 7b	4	0,41	0,34	0,16	Local	82%
Pr 5	3		None		Global	100%
Pr 6	3	0,82	0,64	0,29	Local	54%
Pr 7	3	0,63	0,49	0,29	Local?	63%
Pr 8	2	0,68	0,54	0,25	Local?	57%

4 Comparison

In Fig. 8 the buckling behavior predicted by the solid elements models is compared with the experimental results. It is found that there is generally a good agreement between the predicted buckling behavior and the observed behavior during the experiments, despite the fact that exact boundary conditions of the experiments are not fully reproduced in the FE models.

The numerical analyses give a quite sharp borderline between the local and global buckling modes. For the experiments this borderline cannot be expected to be sharp and the experiments also indicate that there is a band along the borderline where both local and global buckling behavior can be expected. This band seems to be wider as the delaminations get bigger and deeper in the panels. This also agrees with the sub-mode area found for the numerical analyses. However, more experiments and analyses are needed to obtain more solid conclusions on this band.

The reduced compressive strength caused by delaminations in flat UD panels is summarized in Fig. 9, where the results from both FE approaches are compared with experimental data. It is generally found that the reduced compressive strength is larger for the experiments than predicted by the FE-analyses also because of differences in boundary conditions. However, shell element models appear in slightly better agreement.

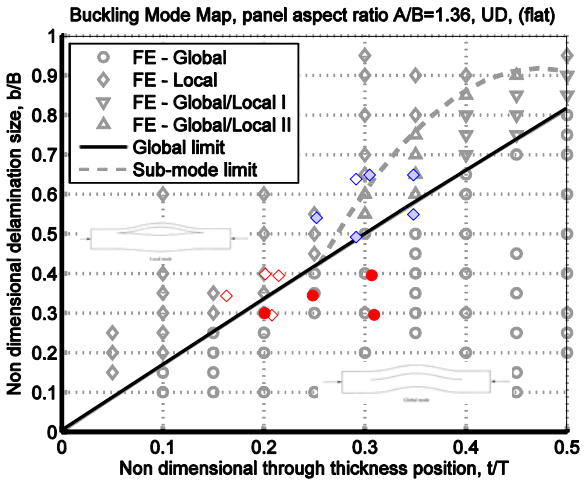

Fig.8. Buckling mode map for flat UD panels with experimental results included. Type ‘In’ panels are red and type ‘Pr’ panels blue. Solid circles mean global buckling while diamonds mean local buckling. The light blue colored diamonds mean that the local behavior is uncertain or the panel sometime shown global behavior.

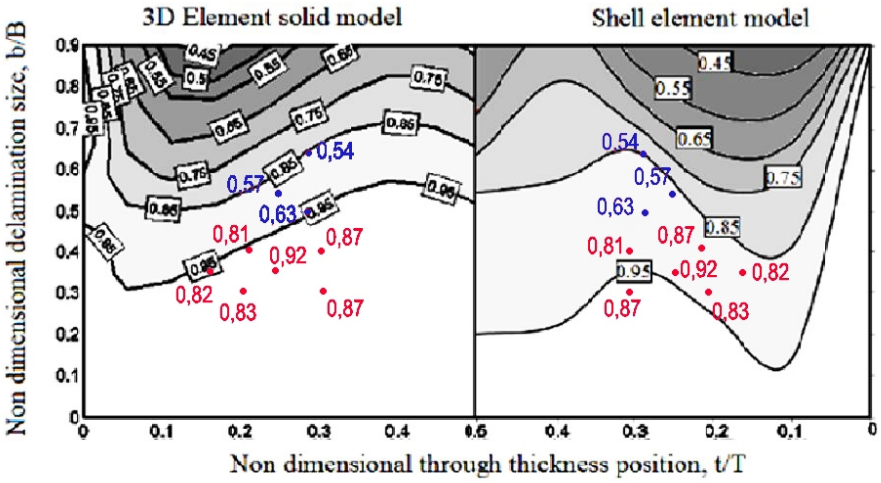

Fig.9. Comparison of reduced compressive strength from tests and numerical analyses: type 'Pr' panels are blue and type 'In' panels are red (points are mirrored with respect to y-axis), curves summarize FE results. Labels show average reduced buckling load factor P_i/P_n from the experiments.

5 Conclusions

Tests results were presented in this paper showing that fabrication method and delaminations affect buckling strength of composite laminates.

Two completely different FE modeling approaches were attempted to simulate their buckling behavior: one adopts 3D elements and implies rather high computational efforts while the other requires less computer resources and it is intrinsically able to catch the local bending behavior at the edges of the delamination.

Comparison of experimental and FE results highlights capabilities and application limits of the proposed models.

Acknowledgments

The work is partly supported by the Danish Agency for Science, Technology and Innovation through the Danish Centre for Composite Structures and Materials for Wind Turbines (DCCSM) (grant no. 09-067212).

References

[1] A.L. Hansen, E. Lund, S.T. Pinho and K. Branner. "A hierarchical FE approach for simulation of geometrical and material induced instability of composite structures". in: *Proc. of 2nd ECCOMAS thematic conference on the mechanical response of composites* (Composites2009), Imperial College London, UK, 2009.

[2] M.L. Bucalem and K.J. Bathe. "Higher-order MITC general shell elements", *Int. J. Num. Meth. Eng.*, 36(21):3729-3754, 1993.

[3] M. Gaiotti, C.M. Rizzo, K. Branner and P. Berring. "Finite elements modeling of delaminations in composite laminates", in: *Proc. of 3rd International Conference on Marine Structures* (MARSTRUCT), 28-30 March 2011, Hamburg, Germany.

[4] S.O. Peck and G.S. Springer. "The behaviour of delaminations in composite plates - analytical and experimental results". *Journal of Composite Materials*, 25:907–929, 1991.

[5] G.J. Short, F.J. Guild and M.J. Pavier. "The effect of delamination geometry on the compressive failure of composite laminates". *Composites Science & Technology*, 61:2075-2086, 2001.

[6] B.F. Sørensen, K. Branner, E. Lund, J. Wedel-Heinen and J.H. Garm. *Improved design of large wind turbine blade of fibre composites (phase 3).* Summary Report, Risø-R-1699(EN), Risø National Laboratory for Sustainable Energy, Denmark, 2009.

[7] B.F. Sørensen, H. Toftegaard, S. Goutanos, K. Branner, P. Berring, E. Lund, J. Wedel-Heinen and J.H. Garm. *Improved design of large wind turbine blade of fibre composites (phase 4).* Summary Report, Risø-R-1734(EN), Risø National Laboratory for Sustainable Energy, Denmark, 2010.